Original article

Institution of MECHANICAL ENGINEERS
Journal of PROCESS MECHANICAL ENGINEERING

Proc IMechE Part E:
J Process Mechanical Engineering
1–12

DOI: 10.1177/09544089221104449
journals.sagepub.com/home/pie
SAGE

Wear behavior of high volume Al_2O_3-reinforced Al7075 matrix composites fabricated by semi-solid powder processing

Saeed Aghajani[1], Vahid Pouyafar[1] and Ramin Meshkabadi[2]

Abstract

The aim of the present study is to fabricate high volume Al_2O_3-reinforced Al7075 matrix composite by semi-solid powder processing method as an effective method to achieve the desired wear properties. The alloy powder (20 μm) was mixed with Al_2O_3 (120 μm) for 10 min and 5 h by planetary ball mill to overcome the powders agglomeration. The wear behavior of the composites was studied using the pin-on-disk tribometer. The effects of milling time, compact pressure, and reinforcement content were investigated to enhance the wear resistance. The results of the tribotests indicated that composites with coarser reinforcing particles (lower milling time) have good wear resistance. The role of compaction pressure in highly loaded composites is remarkable. The maximum wear resistance was observed for the 50% Al_2O_3 composite. The wear resistance increased as the reinforcement volume increased before reaching a critical value. Abrasive wear is the predominant mechanism in the wear of reinforced composites containing less than the load limit. However, adhesive and laminating wear are the controlling mechanisms at overloads. The results indicate valuable information in the development of aluminum-based composites.

Keywords

Al7075/Al_2O_3 composite, semi-solid powder processing, highly reinforced Al_2O_3, wear properties

Date received: 10 November 2021; accepted: 18 April 2022

Introduction

Aluminum alloys are lightweight and good conductors of heat and electricity, but they have low wear resistance. For this reason, the use of reinforcements is of high necessity.[1,2] Aluminum-based composites with hard ceramic particles like SiC, Al_2O_3, TiC, and B_4C are used to meet the needs of the military, automotive, and aircraft industries. They have a wide range of applications due to their strength, modulus of elasticity, high wear resistance, and various manufacturing methods. Aluminum-based composite parts, such as brake rotors, are subjected to wear and slipping on each other during the operation.[3] For this reason, it is crucial to study their tribological behavior and enhance their wear resistance.[4,5]

Among the variety of manufacturing processes available for high volume reinforced composites, semi-solid powder processing (SPP) produces components with complex geometry in fewer forming steps compared to other forming techniques. It develops the semi-solid forming by replacing the bulk material with powdered material, which enables the utilization of powder metallurgy.[6] This method has been successfully applied in processing aluminum-based composite materials, with SiC[7] and CNT[8] reinforcements. It allows the combination of different powders to improve the properties and eliminate post-processing operations using the flow characteristics and microstructural properties of semi-solid materials.[9] Liu et al. investigated the wear behavior of A356 alloy produced by both traditional and semi-solid casting methods. The semi-solid casting process improved the alloy wear compared to conventional casting.[10] Radha et al. investigated the mechanical and the wear behavior of Al7075/B_4C/Gr composites prepared by stir casting. They showed that the hybridization of two reinforcements enhances the wear resistance, especially at the high sliding speeds.[11] Yaping et al. investigated the effect of Al_2O_3 particles on the mechanical and wear behavior of 7075 aluminum alloy. The tribological properties showed that 5 wt.% Al_2O_3 significantly improved the high-temperature wear resistance of the alloy.[12] Essa et al. investigated the tribological properties of M50 alloy steel reinforced with ZnO and MoS_2 solid lubricants at

[1]Manufacturing Engineering Department, University of Tabriz, Tabriz, Iran
[2]Department of Engineering Sciences, Faculty of Advanced Technologies, University of Mohaghegh Ardabili, Namin, Iran

Corresponding author:
Vahid Pouyafar, Manufacturing Engineering Department, University of Tabriz, Tabriz, Iran.
Email: pouyafar@tabrizu.ac.ir

high temperatures. They showed that the composite containing both additives had the least friction and good lubricating behaviors were obtained.[13] In another study, Ali and Xianjun sintered M50 alloy steel by spark plasma sintering (SPS) and studied their tribological properties using a pin-on-disk tribometer. The results showed that M50 alloy steel reinforced with TiO_2 and graphene (G) had excellent wear properties compared to the base material.[14]

High volume fraction reinforcement metal matrix composites (MMCs) are very popular due to their desirable mechanical and thermo-physical properties. In recent years, researchers considered various manufacturing methods for these materials.[15–19] He et al. synthesized Mg matrix nanocomposite with high volume fraction SiC reinforcement via mechanical alloying followed by SPS.[16] Prabhu et al. synthesized Al–Al_2O_3 MMC with volume fractions of 20%, 30%, and 50% Al_2O_3 by high-energy milling of the blended component powders. A uniform distribution of the Al_2O_3 reinforcement in the Al matrix was successfully obtained.[18] Zheng et al. prepared Al alloy matrix composites reinforced by a high volume fraction of B_4C particles by the powder metallurgy method.[19]

In recent years, a few studies have been conducted on the wear properties of the materials fabricated by the SPP method compared to casting or powder metallurgy. Alhawari et al. made A359/Al_2O_3 composite using stir casting and semi-solid processing methods. They used a pin-on-disk tribometer to perform wear tests. The results showed that the volume loss of the composites produced by semi-solid processing was lower than that of those produced by conventional casting.[20]

The objective of the present study is to prepare composite powder with a uniform dispersion of high volume fraction reinforcing phase and then manufacture a sample by the SPP method as an effective method to achieve the desired wear properties. Studies on the wear resistance of various materials show that the alloys and composites made by the semi-solid processing have better wear properties than other methods.[21] Homogeneous distribution of the reinforcing phase and their tendency to agglomeration is another challenge in the preparation of nanocomposites with high reinforcement volume and nanoscaled. This could be overcome using a high-energy planetary ball mill in the preparation of primary powders. Therefore, the effects of fabrication parameters and wear test conditions on the wear resistance of the manufactured nanocomposites are studied in this paper. Considering the advantages of the SPP method, it is worth studying the manufacturing process and wear behavior of these composites.

Materials and methods

A planetary ball mill and a mechanical stirrer (NARYA-MPA-2*250, Amin Asia Company, Iran) were used to mix the powders of pure aluminum with a particle size of 20 μm and other elements of Al7075 alloy (Khorasan Powder Metallurgy Company, Iran), as shown in Table 1. To mix Al7075 powder with Al_2O_3 particles with an average particle size of 120 μm (Iran Alumina Company, Iran) as reinforcement in 40%, 50%, and 60% volume, a high-energy planetary ball mill with a rotational speed of 250 r/min was used. Cylindrical mill chambers were made from polyamide and contained steel balls. The balls' diameters were 10 and 15 mm and their ball-to-powder weight ratio (BPR) was 5:1. The prepared composite powders were milled at two different milling times (10 min and 5 h) and dried in the air. The milling time of 10 min was selected as a short and the time of 5 h as the long milling time to study the powders' morphology, their changes, and their effect on the size of the reinforcing phase as well as wear properties. Stearic acid (1 wt.%) was used as a process control agent to prevent cold welding and agglomeration.

Table 1. Elemental 7075 powder constituents.

Element	Al	Zn	Mg	Cu	Cr	Fe	Si	Mn
Content (wt.%)	Balance	5.6	2.5	1.5	0.23	0.2	0.1	0.1

Determining the appropriate temperature for SPP

For sample fabrication, 12 g of mixed powder was poured into the dye. The dye was placed inside an induction furnace under a screw press to apply pressure. An initial pressure of 5 MPa was applied to compact the powder. The samples were heated up to semi-solid temperatures of 575, 585, 595, 605, 615, and 625°C. The proportional liquid fraction to the above temperatures from differential scanning calorimetry (DSC) analysis equals 8%, 14%, 20%, 31%, 42%, and 60%, respectively (Supplementary Figure 1). Upon reaching the abovementioned semi-solid temperatures, the pressure was applied slowly up to 100 MPa, and the samples were compressed for 45 min to equilibrate the liquid phase and form a homogeneous structure.[22,23] This is the time to establish a thermal balance between the powder particles to bond with each other. Finally, the pressure was removed slowly and the product was cooled inside the furnace. Figure 1 shows a schematic of the utilized set-up in the process with its various parts. The dye material was L316 stainless steel.

Friction between the powder particles and the dye wall leads to a reduction in the dye life, increases the likelihood of defects in the workpiece, and most importantly, reduces the part's density. For this purpose, a lubricant (MoS_2) is used to reduce the friction between the powder particles and the dye wall.

The purpose of preparing samples of Al7075 powder at this stage is to determine the appropriate semi-solid temperature based on the desired mechanical properties. Also, the obtained physical and mechanical properties will be compared with the properties of the samples prepared from the composite powder in the next section.

The SPP of the reinforced powder is similar to the method explained in Section 2.1, except that the semi-solid

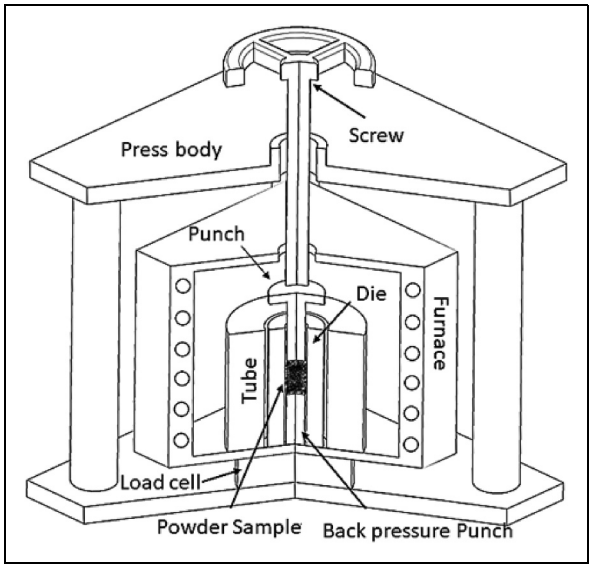

Figure 1. Experimental setup of the SPP.
SPP: semi-solid powder processing.

temperature is the specified optimum one. The compression was performed under two different pressures (50 and 100 MPa).

Performed tests

Scanning electron microscopy (SEM) model MIRA3-FEG-SEM made by TESCAN Co. (Czech Republic) examined the morphology and microstructure of samples. Elemental analysis by the D5000 X-ray powder diffraction system made by Siemens was used to identify powder compounds in the specific points of the samples. The Shimadzu pressure device (model AG-25TB) with a speed of 1 mm/min was used to measure the compressive strength. The density of samples was measured using the Archimedes principles. Since the presence of porosity inside the material affects the wear properties and increases its wear rate, it is necessary to calculate the volume percentage of porosity in the produced samples from equation (1).[14]

$$Porosity(\%) = 100 - \left(\frac{Sintered\ density}{Theoretical\ density} \times 100\right) \quad (1)$$

The theoretical density was calculated according to the "rule of mixtures" using equation (2).

$$\rho_{T/Al7075} = \frac{1}{\left(\begin{array}{l}\frac{wt\%Al}{\rho_{Al}} + \frac{wt\%Zn}{\rho_{Zn}} + \frac{wt\%Mg}{\rho_{Mg}} + \frac{wt\%Cu}{\rho_{Cu}} \\ + \frac{wt\%Cr}{\rho_{Cr}} + \frac{wt\%Fe}{\rho_{Fe}} + \frac{wt\%Si}{\rho_{Si}} + \frac{wt\%Mn}{\rho_{Mn}}\end{array}\right)} \times 100 \quad (2)$$

The manufactured Al7075–40% Al_2O_3 composite had a theoretical density of 2.81 g/cm^3 and sintered density of 2.76 g/cm^3. Therefore its porosity content is 1.77 (vol.%). On the other side, the theoretical and sintered densities of Al7075 are 2.71 and 2.60 g/cm^3, accordingly resulting in a porosity content of 4.05 (vol.%). It is seen that adding Al_2O_3 reinforcement decreases the porosity content.

Table 2. The microhardness of manufactured frictional samples.

Experiment condition Reinforcement (vol.%)	5 h milled, 100 MPa	10 min milled, 100 MPa	5 h milled, 50 MPa	10 min milled, 50 MPa
	Hardness (HV)			
40	198.20	186.13	102.53	89.81
50	167.00	159.02	72.16	66.23
60	130.03	96.62	54.17	47.92

The Vickers hardness of high loading composites was studied using the SCTMC micro Vickers hardness tester model HV-1000 by applying 5 N load and holding it for 15 s. The reported values are shown in Table 2, representing the average of four measurements.

For wear resistance, the dry sliding wear test was performed at ambient temperature with a pin-on-disk tribometer according to ASTM G99-17 standards.[24] Samples with a diameter of 10 and a height of 15 mm were machined. The cross-sectional area was ground up to 2000 grit, achieving a primary average surface roughness (Ra) of 0.8 ± 0.02 μm. All samples were prepared under the same conditions in terms of surface morphology and surface roughness. Before the experiment, the sample weight was measured with an accuracy of 0.1 mg. The abrasive plate was made of cold work tool steel (DIN 1.2080) and hardened to 62 Rockwell C (RC). Before testing and weighing, the surface of the samples and the abrasive disk were thoroughly cleaned with acetone. All specimens were ground to a fixed diameter of 200 mm. The schematic of the process is shown in Supplementary Figure 2.

Various criteria are considered to investigate the wear behavior of materials, including wear rate, surface roughness, coefficient of friction, and other related parameters. It is concluded from the results of an investigation by Essa et al. that the friction coefficients and wear rates have similar behaviors for all examined conditions when studying the tribological properties of M50-steel-based composites.[13] In the present study, the wear rate has been used to investigate the wear behavior. It is used as a precision indication of the wear behavior of the Al7075–SiC composite through the design of experiments to optimize the process parameters.[25] Wear resistance is obtained using the ratio of the volume of lost material to the traveled distance. The lost volume is calculated by dividing the weight difference before and after wear over the sample density. In equation (3), WR indicates the wear rate. After each test, the surface of the sample was cleaned with acetone and weighed.

$$WR\left(\frac{mm^3}{m}\right) = \frac{Mass\ loss\ (mg)}{Density\left(\frac{g}{cm^3}\right) \times Distance\ (m)} \quad (3)$$

The wear tests were performed in two modes. In the first mode, the cylindrical samples slid a constant distance of 2 km under applied forces of 10, 20, 30, and 40 N. In the second case, the abrasive pins were worn at a constant force of 20 N at distances of 1, 2, 3, and 4 km. The rotational speed of 300 r/min was considered the same for all samples. As is known, The ASTM G99-17 standard does not specify the amount of loads and the results of the wear test have comparative values. In this study, the loads and rotational speed are based on the general industrial operation of parts and not on specific applications. So, the values of loads and rotational speed have been selected from the previous research on the studied composite material.[26,27] The variable parameters of the fabrication process, as well as the wear tests, are summarized in Table 3. For each of the compression test, relative density, and wear test, three samples were tested to obtain reliable results and their average was reported.

Table 3. Parameters and values.

Parameter	Value
Milling time	10 min and 5 h
Reinforcement volume (%)	40, 50, and 60
Compact pressure (MPa)	50 and 100
Wear force (N)	10, 20, 30, and 40
Wear distance (km)	1, 2, 3, and 4

Results and discussion

Al7075/Al2O3 powder morphology

The powder morphology has a direct effect on the microstructure and the wear properties of the fabricated parts. Comparing the morphology of the powders before (Figure 2(a)) and after ball milling (Figure 2(b), (c)), the deformation and smoothing of aluminum particles are observed due to the impacts inside the ball mill. The particle size of the matrix phase remains almost unchanged.

The way composite powders are prepared affects their morphology. By mixing the powders in a short time (10 min), little change is seen in the matrix and reinforcements morphology (Figure 2(b)). Therefore, the alloying operation is not completed, and only the reinforcing particles are distributed among the matrix phase. After 5 h, the aluminum phase is deformed and changed to a laminar morphology. The particles accumulated on top of each other and coaxial particles are formed due to the continuous welding.[28] It can be seen that the particle distribution is well done in 5 h, but little coaxial particles are formed, and they are shaped irregularly (Figure 2(c)).

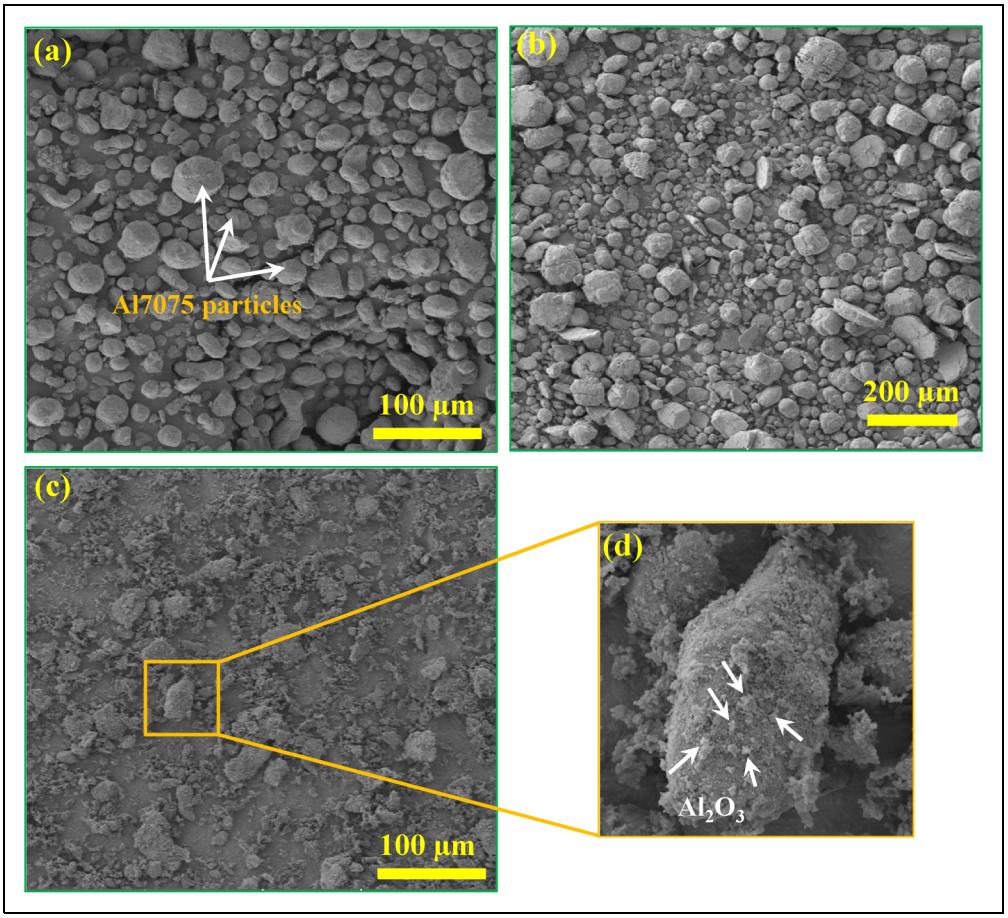

Figure 2. The powder morphology of (a) Al7075 powder, the ball-milled Al7075–40% Al_2O_3 powder for (b) 10 min, and (c) 5 h and (d) magnified Al particle with Al_2O_3 particles.

Despite the tendency of aluminum particles to the deformation and cold welding, in composites with a high percentage of Al_2O_3, brittle alumina particles prevent them from welding by crushing and adhering to the surface of the deformed aluminum (Figure 2(d)). Thus, irregularly shaped particles are formed.

As the milling time increases, coarse and brittle particles of the reinforcement are crushed due to the microcracks arising from collisions within the ball mill. At the same time, the Al_2O_3 particles are deformed, and their size decreased to about 1 µm from 120 µm after 5 h (Supplementary Figure 3). Such a reduction in ceramic particle size leads to morphological changes.[29] Regarding the distribution of the reinforcement phase between the matrix phases, it can be said that the distribution of composite particles is uniform in both milling times, but in 5 h of milling, alumina particles with an approximate size of 1 µm are formed and attached to the surface of the aluminum particles during milling (Figure 2(c)).

The appropriate semi-solid temperature for SPP

The appropriate semi-solid temperature for making Al7075/Al_2O_3 composite was investigated by evaluating the physical and mechanical properties of the samples. To this end, the relative density and compressive strength of the fabricated samples were determined and shown in Figure 3. It is observed that with increasing semi-solid temperature, the relative density of the alloy increases and reaches its maximum value in the temperature range of 615–625°C. Besides, the compressive strength increases with increasing semi-solid temperature. With a further increase of the temperature to 625°C, the compressive strength decreases a little due to the growth of primary grains. At lower temperatures, because of the lack of liquid phase, the primary particles are bonded together to form large grains under pressure. The obtained results are in line with previous research reported by Chen et al.[30]

Figure 3 indicates a high increase in compressive strength and relative density between 575 and 585°C. This is due to the slope of the liquid fraction against temperature in the alloy DSC curve as shown in Supplementary Figure 1. In this figure, it is observed that the rate of liquid fraction increase in the range of 575–585°C is lower than the subsequent temperatures and the liquid fraction in the alloy has slightly changed. The higher the temperature than 585°C, the higher the rate of increase in the liquid fraction and the lower the mechanical and physical properties of the sample.

The microstructure shown in Figure 3 corresponds to a compacted alloy at 615°C with a compaction pressure of 50 MPa. Small- and medium-sized spherical grains surrounded by the liquid phase are formed without any space between the particles. It is concluded that a suitable increase in the semi-solid temperature is very beneficial to achieve the ideal semi-solid structure.

Despite the increase in the relative density of the alloy with increasing semi-solid temperature, the resultant increase in the liquid phase to more than 50% makes the distribution of liquid and solid phases heterogeneous. Segregation of liquid and solid phases leads to melting leakage and agglomeration of solid particles. This phenomenon in composites leads to the agglomeration of reinforcements at lower mold levels. For this reason, the suitable temperature for making 7075 aluminum-based composites is 615°C, with the liquid phase corresponding to this temperature being approximately 40%. This fraction prevents the liquid phase from escaping the solid grains and forms a solid phase with irregular morphology in the semi-solid compression stage.[31]

Wear properties

The effect of composite fabrication parameters. Wear characteristics of Al7075/Al_2O_3 composite fabricated by SPP depend on particle size and semi-solid compaction pressure. Figure 4 shows the wear rate of 40% Al_2O_3 composite under different fabrication conditions. As the semi-solid compact pressure increases from 50 to 100 MPa, the wear rate of the milled sample for 5 h decreases from 0.93×10^{-3} to 0.45×10^{-3} mm^3/m

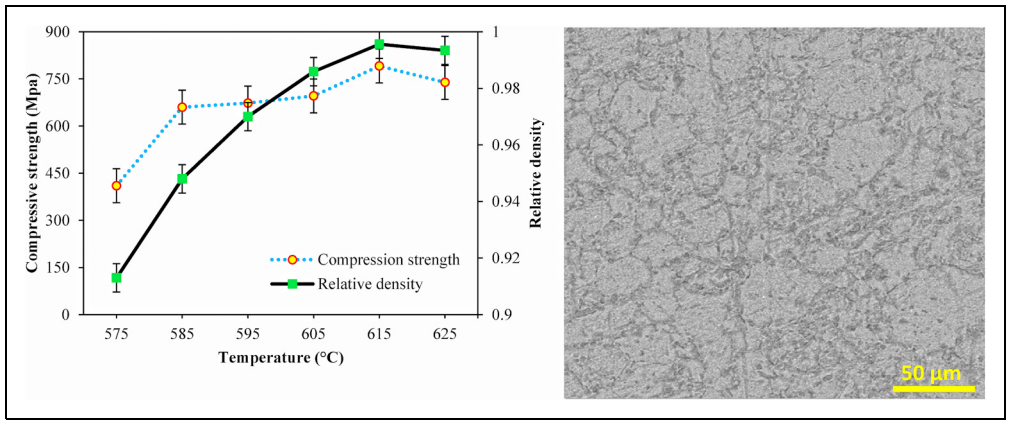

Figure 3. Relative density and compressive strength of Al7075 at semi-solid temperatures and microstructure of Al7075 compacted at 615°C under 50 MPa.

(52%). Also, the wear rate for the milled specimen for 10 min is reduced from 0.75×10^{-3} to 0.25×10^{-3} mm^3/m (66%). By increasing the compaction pressure, the liquid phase flows better and fills the existing cavities.

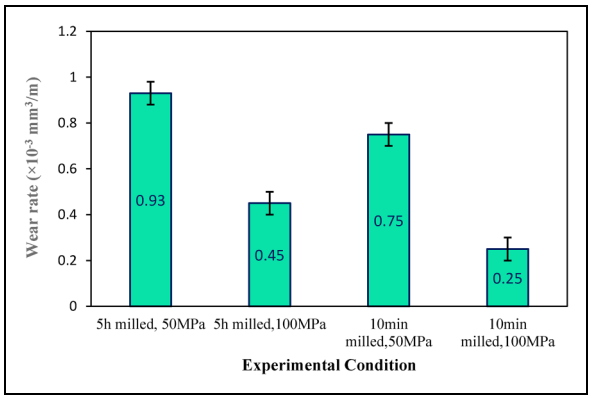

Figure 4. Wear rate of the 40% Al_2O_3 composite under different fabrication conditions (applied force of 20 N at a distance of 2 km).

Therefore, the relative density of the specimen increases, which leads to a decrease in wear rate.

Reinforced composites milled for 10 min have better wear resistance than milled samples for 5 h. As mentioned earlier and shown in Figure 2, the milling process affects the shape and size of the particles so that the large Al_2O_3 particles are crushed by the impact of balls. Larger reinforcing particles (120 μm) protect the matrix better than finer particles (1 μm) and have higher wear resistance. Reducing the reinforcing particles' size (higher milling time) and transferring the applied forces to them resulted in reducing the wear resistance.

Figure 5 shows the wear surface of 40% Al_2O_3 composite samples. The wear surface of all samples consists of white areas, indicating cavities, and black areas, indicating a mechanically mixed layer (MML). These areas are marked with the letters A and B, respectively. In compacted samples at 50 MPa (Figure 5(b) and (d)), the porous areas are more than the MMLs. Poor bonding of the base metal with the reinforcement particles at a low compact pressure removes the fine and coarse Al_2O_3 particles. These areas for composites made with 10 min of

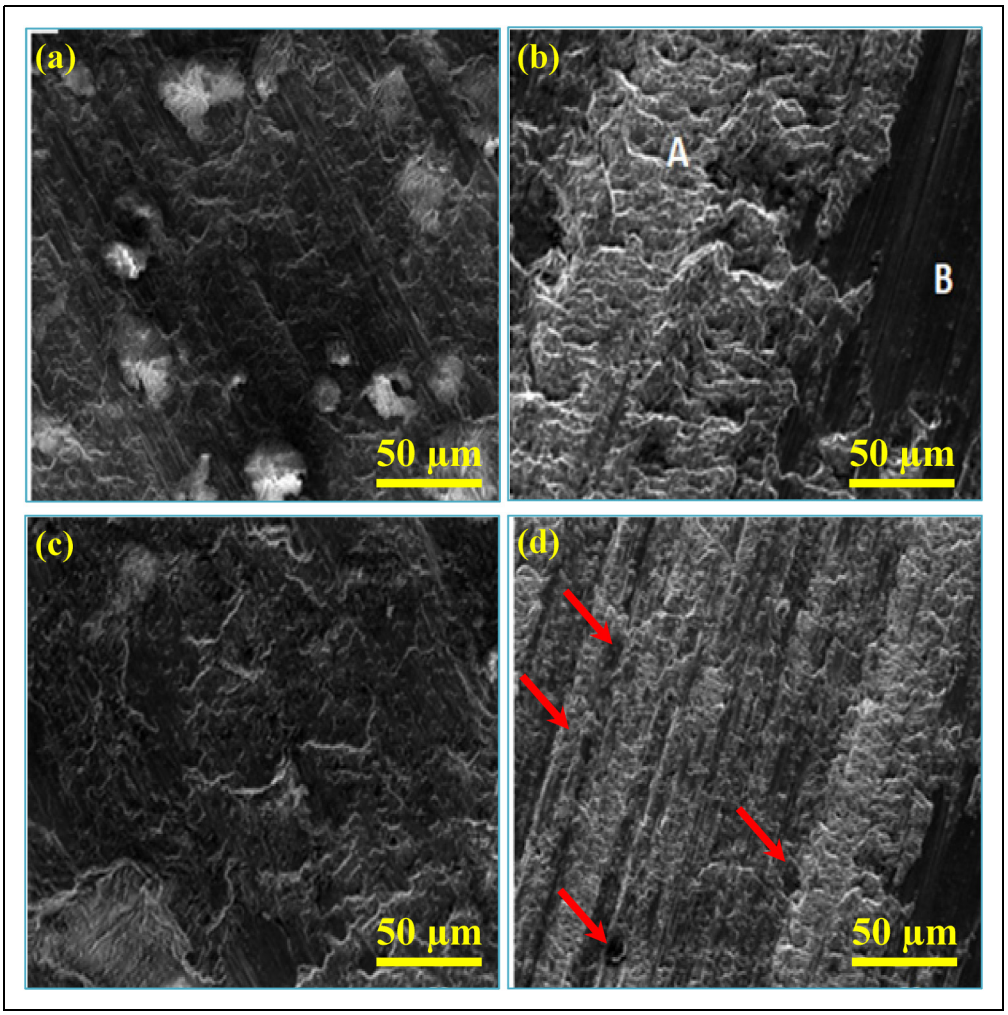

Figure 5. Wear surfaces of composites (wear force of 20 N and distance of 2 km) in different fabrication conditions (a) P = 100 MPa, t = 10 min, (b) P = 50 MPa, t = 10 min, (c) P = 100 MPa, t = 5 h, and (d) P = 50 MPa, t = 5 h.

milling time (Figure 5(a) and (b)) are less than composites made with 5 h of milling time (Figure 5(c) and (d)).

Scratches parallel to the direction of wear are not continuous in all specimens and are limited to the black areas marked with the letter B. Zone B has experienced a layered deformation and has become a valley due to the separation of the reinforcement from the matrix phase. Not only are the scratches on composites made with 10 min of milling time (with larger reinforcing particles) lower (Figure 5 (a) and (b)), but also the number of valleys is small. This can be due to the strong bonding of Al_2O_3 particles to the matrix phase. It can be concluded that the protection of coarse particles from the matrix is more and increases the wear resistance of the composite. The increased force on the particles leads to the removal of fine reinforcing particles after a certain distance. This is the distance at which the applied force overcomes the bond between the reinforcing particle and the matrix phase. For this reason, large particles have better wear resistance than fine particles. This conclusion is in line with the findings of the research of Al-Rubaie.[32]

Examination of Figure 5 indicates that lower pressures cannot create a strong bond between Al_2O_3 particles and aluminum. The lack of required force for the liquid phase to flow between the reinforcing particles is the reason. Therefore, at low pressures, Al_2O_3 particles are placed very loosely next to each other in the matrix phase. By applying a load in the wear test, these particles are separated after a certain length. The areas displayed by the red arrows in Figure 5(d) show the removal of the reinforcing particles. These results show the importance of compact pressure in highly reinforced composites. The generated heat by the wear test softens these composites, and adhesive wear occurs. Plastic deformation and layering of the surface are considered the prime wear mechanism of these composites.

The effect of Al_2O_3 volume. The wear resistance increases with the increasing Al_2O_3 percentage. This is related to the increase in the hardness and strength of materials, which is in line with the Archard equation. Figure 6 shows the wear rate changes against reinforcement content at a pressure of 100 MPa, milling times of 10 min and 5 h, an applied force of 30 N, and a distance of 2 km. Increasing the Al_2O_3 percentage from 40% to 50% decreases the wear rate, but as the reinforcement phase increases from 50% to 60%, the wear rate increases. For a highly loaded Al_2O_3, the maximum wear resistance is observed in the 50% Al_2O_3 composite. As shown in the figure, with increasing Al_2O_3 percentage from 40% up to 50%, the wear rate for both types of composites with different milling time decreases.

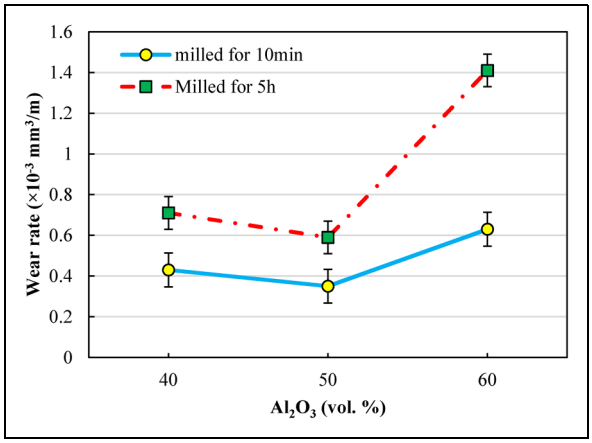

Figure 6. Wear rate changes in terms of Al_2O_3 content (compact pressure of 100 MPa, applied force of 30 N, and wear distance of 2 km).

Figure 7 presents the SEM images of the wear surfaces according to the conditions of Figure 6. The hardness of aluminum is less than the abrasive disc, so separation from the alloy surface occurs. As a result, smooth surfaces and more tribolayers are found in Al7075 unlike the cavities and micro-grooves in the worn surface of the reinforced Al7075 alloy (Figure 7(a)). These grooves are due to abrasive wear which is caused by the trapping and rolling of separated alumina particles between the disk and samples, and their dimensions vary with the reinforcement percentage (Figure 7(b), (c), and (d)). The number of grooves in the 50%-Al_2O_3 composite (Figure 7(c)) is less than the rest. Therefore, the MML layer and the reinforcing particles increase the composite wear resistance. These characteristics of reinforcing particles depend on their loading limits to the composites. As seen in Figure 7(d), the wear surface of the 60%-Al_2O_3 composite is different and most of the reinforcing particles are separated from the matrix phase due to the lower bond strength.

It is known that reinforcement geometry, total contact area, and bonding strength between the composite matrix and reinforcement phases affect the mechanical properties of the composites.[33,34] When Al_2O_3 was high (60 vol. %), these particles act as barriers and there was not sufficient Al7075 phase to completely infiltrate into the porous network formed by the Al7075 phase. Therefore, the bonding strength between reinforcement and matrix phase becomes weaker as the Al_2O_3 increases by more than 50% which is the maximum loading limit.

As shown in Figure 2(c), 5 h milled powders have agglomerated Al_2O_3 particles on deformed Al7075 particles which cause poor bonding of the reinforcement and matrix particles and lowered bonding strength of the samples. As a result, a sudden change in the wear rate of these composites occurred in reinforcement fractions more than the loading limit of 50% (Figure 6).

The effect of wear force and distance. Figure 8 shows the wear rate changes against applied force during a slip length of 2 km. It is observed that with increasing the force, the wear rate of composite increases. By increasing the force, the penetration depth of abrasive particles increases, and the continuation of the abrasion process leads to the formation of grooves and separation of the material from the surface. The effect of Al_2O_3 content at higher forces is also visible. It is observed that at higher forces, samples reinforced with large particles

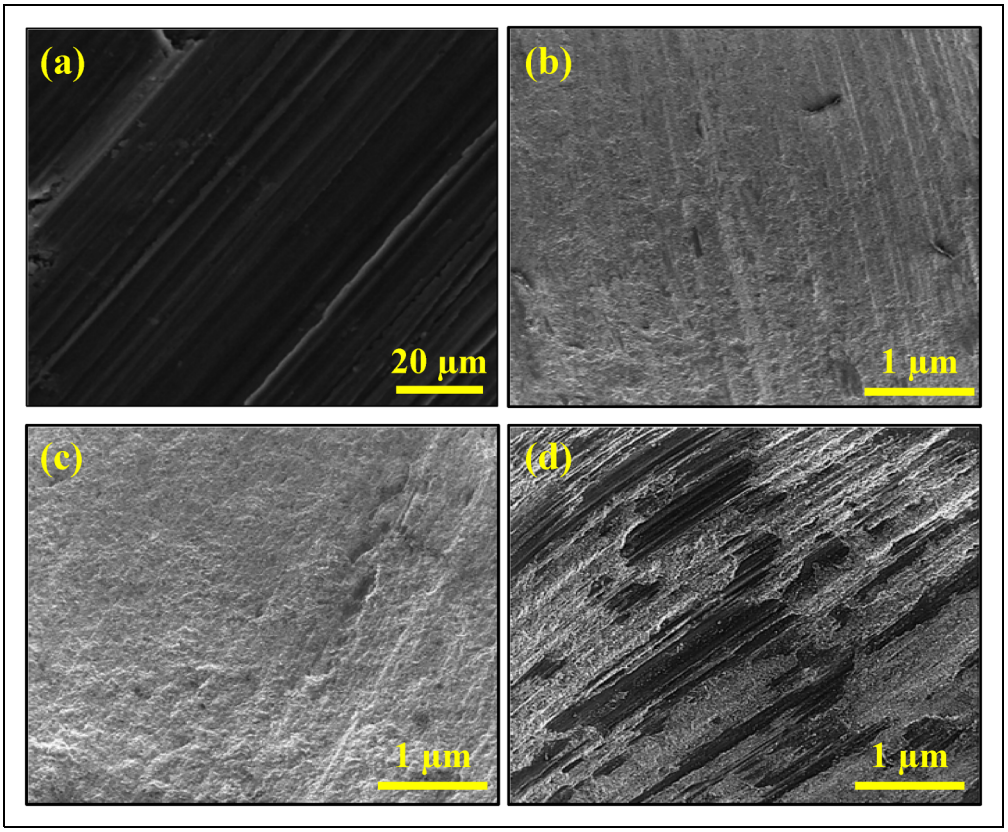

Figure 7. SEM images of the wear surfaces (a) base alloy and composites containing (b) 40, (c) 50, and (d) 60% Al_2O_3 (compact pressure of 100 MPa, applied force of 30 N, and a distance of 2 km).
SEM: scanning electron microscopy.

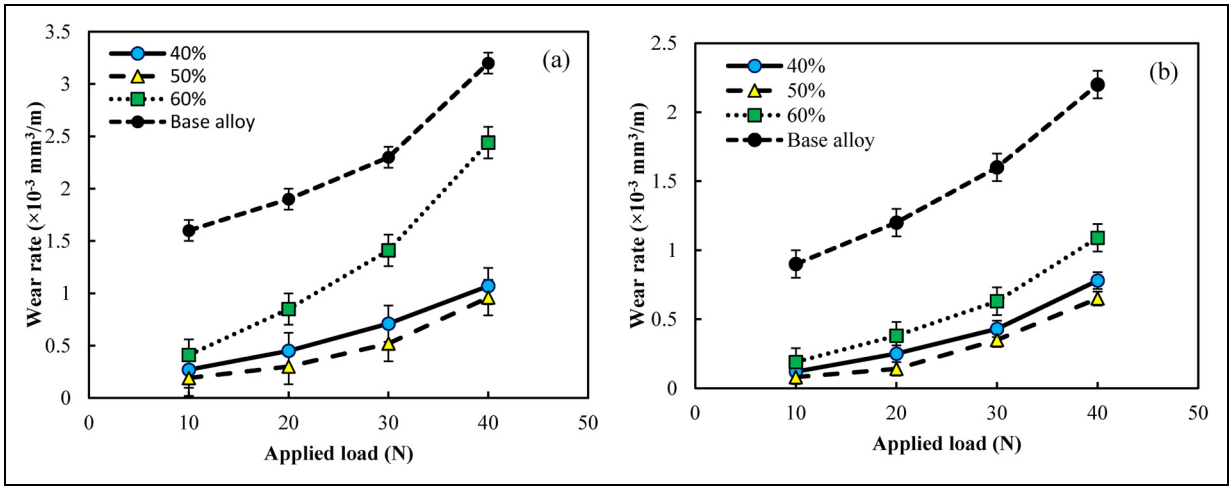

Figure 8. Wear rate changes against wear forces at different milling times (a) 5 h and (b) 10 min (compact pressure of 100 MPa and distance of 2 km).

(Figure 8(b)) show better wear resistance. On the other hand, in composites with finer reinforcing particles (Figure 8(a)), the wear rate is almost linearly related to the increase in applied force for 40% and 50% Al_2O_3, while in the case of 60% Al_2O_3, this increase occurs suddenly.

The wear surfaces of 50% Al_2O_3 composite samples under forces of 10, 20, 30, and 40 N are shown in Figure 9. By examining the microstructure, it is possible to see the changes in the wear mechanism due to the increase in force. Al_2O_3 particles are seen on the surface of the worn sample under an applied load of 10 N, which indicates good bond strength between the particles. The wear mechanism is of surface oxidation type. The separated abrasive particles are fractured, milled, oxidized, and eventually adsorb into the base metal. In this case, an MML is formed on the sample's surface (Figure 9(a)). The MML layer is rich in iron and small

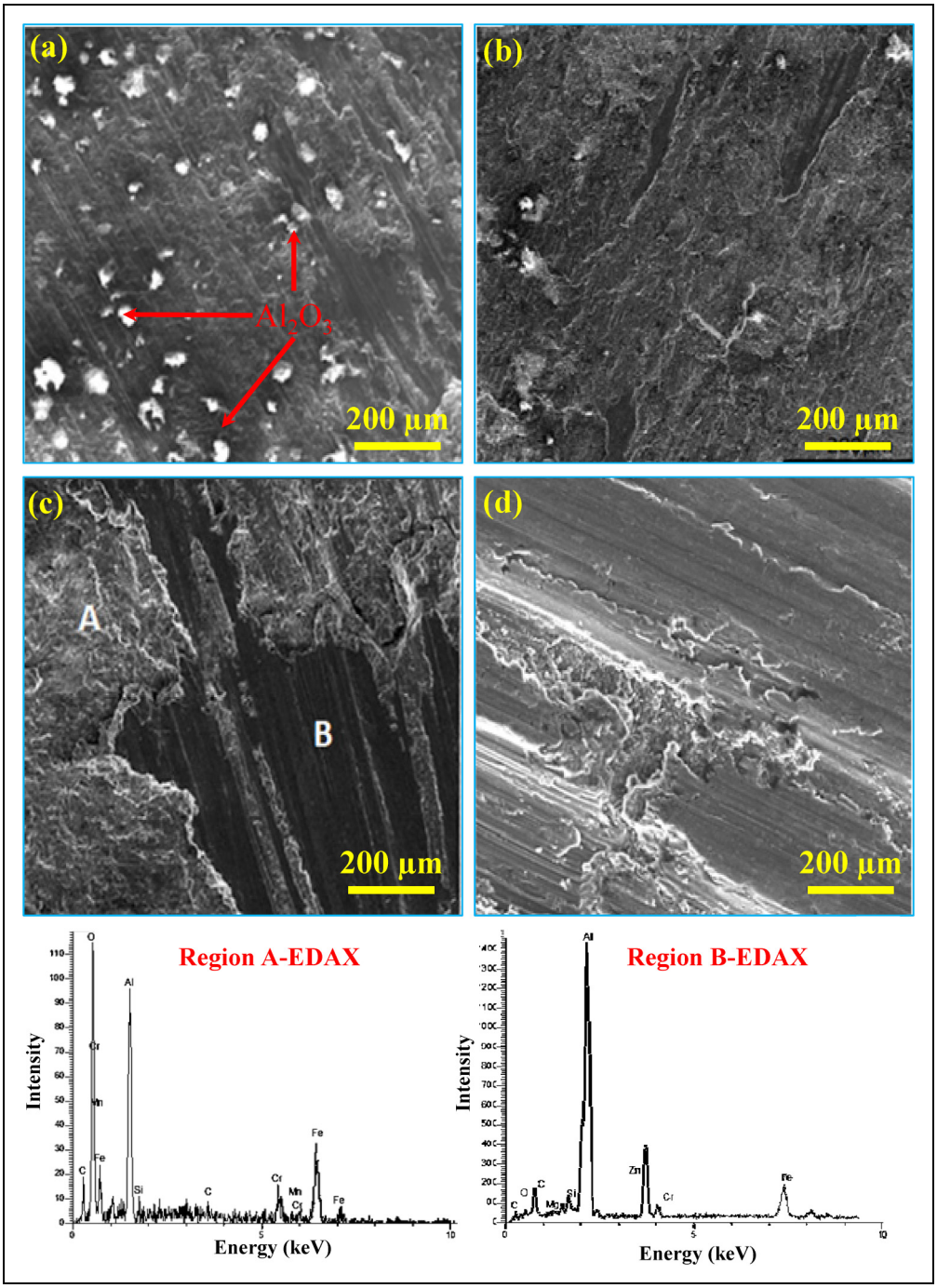

Figure 9. Wear surface of 50% Al_2O_3 composite in a wear distance of 2 km and force of (a) 10, (b) 20, (c) 30, and (d) 40 N (compact pressure of 100 MPa and 10 min of milling) and EDAX analysis of regions A and B of Figure 9(c).

particles of Al_2O_3, evenly distributed inside. This layer helps to increase the wear resistance of the composite at high distances.

As the applied force increases, the MML region becomes thicker so that the smooth black surface of the sample is more in Figure 9(b) compared to Figure 9(a). In this case, the reinforcing particles along with the MML region protect against wear. The wear mechanism is the scratch type and partial layering of the surface is due to the increasing MML thickness. With increasing the force to 30 N, the thickness of the MML layer increases (Figure 9(c)). The small cracks created on the surface have increased because of increasing the applied force and MML thickness. The wear mechanism is a severe laminating mechanism that will become a severe plastic deformation and adhesive abrasion as the process continues. The energy dispersive X-ray analysis (EDAX) analysis of the white (A) and black (B) areas is shown in Figure 9(c). Investigation of the percentage of elements indicates the presence of iron and carbon as separated particles in these areas. Although the percentage of iron in the surface decreases with increasing applied force, in all cases, the amount of iron in region A is relatively more than that in region B.

As the formation of MML increases, the cracks formation and propagation increase the separation of material from the sample's surface. Hence, the three-dimensional wear mechanism for the sample leads to a decrease in wear resistance (Figure 9(d)).

For 60% Al_2O_3 composites, the cracks occur at lower applied forces than other composites, where at a force of 20 N, the MML layer is filled with cracks. As the traveling distance increases, the sample's surface is layered and separated due to the adhesive wear (Supplementary Figure 4). The same procedure happens with unreinforced alloys. Despite the similarity of the wear mechanism for unreinforced alloys with highly loaded composites, the wear resistance of reinforced composites is still higher due to the presence of reinforcing particles.

Thoroughly, under higher vertical loads and long distances, the adhesive mechanism occurs due to ups and downs between the two surfaces. The results obtained for highly loaded composites are in line with previous research on the wear of composites containing low reinforcement content, which indicates that with increasing the reinforcement, wear resistance increases.[35,36]

Wear mechanism. The wear mechanism changed from adhesive–abrasive base alloy to the soft-mild adhesive regime with increasing the Al_2O_3 content. However, the reinforcement loading of 50% indicates the wear mechanism changes from soft-mild adhesive to almost severe wear. This behavior change is completely clear in the comparison of 40% Al_2O_3 composite wear behavior with 60% Al_2O_3. Therefore, the relationship between the wear resistance and wear mechanism depends on the bonding strength of the reinforcement particle by the matrix. SEM micrographs of Figure 7 show shallow scuffs in the sliding direction of 40% and 50% Al_2O_3 while in the samples of the base alloy and 60% Al_2O_3, serious grooves can be seen parallel to the sliding direction.

For the 60% Al_2O_3 sample in Figure 7(d), it is apparent that the MML has not only formed but also deformed and damaged more severely compared to other samples. The removed sections of the MML for 60% Al_2O_3 can be seen in this image. By increasing the normal load, the severity of deformation has been enhanced and hence, the MML which is on the free surface has freely flowed and compacted to lower thicknesses.[37] By increasing the load up to 40 N, MML thickness has caused the wear rate to increase noticeably in both the base alloy and 60% Al_2O_3. In fact, as much the energy transferred to the surface increases, the deformation, MML formation, delamination, and volume loss increase correspondingly. In other words, by increasing the normal load, the volume of lost material increases at constant distances. This result has been confirmed by several researchers about various materials.[38,39]

The wear resistance of the composites is basically related to the wear resistance and hardness of the particles, and not dependent on their bulk hardness. However, this effect is different for various milling times which change the particles' size. The ball-milled samples for 10 min resist on penetration because of their larger size, higher hardness, and good bonding with the matrix. Moreover, the large particles bear most of the wear load. In this case, the surface hardness of the composite is mainly a result of the hardness of the Al_2O_3 particles. Under the sliding wear testing conditions, the main wear mechanism for the composites contains small particles in micro-cutting and micro plowing, whereas it is grinding for the composites containing large particles.[22]

Conclusions

In this research, the SPP method was used to make a highly reinforced Al7075/Al_2O_3 composite. Main conclusions drawn were as follows:

1. Increasing the compact pressure and using powders with less milling time led to a reduction in wear rate. The role of compaction pressure in highly loaded composites is very noticeable. Microstructural examination of the samples in terms of porosity and MML layer confirmed the result.
2. The maximum wear resistance was observed for the 50% Al_2O_3 composite. The MML layer on the wear surfaces and the reinforcing particles increased the composite wear resistance. The low wear resistance of 60% Al_2O_3 composites indicated that the reinforcements are overloaded under these conditions.
3. Abrasive wear was the predominant mechanism in the wear of 40% Al_2O_3 composites. The wear surface of the reinforced composite with 60% Al_2O_3 showed an adhesive–abrasive wear mechanism. Wear resistance depends on the powder's morphology in addition to the hardness of the material. The wear mechanism affected the particles by separating them with a weak bond from the matrix.
4. Al_2O_3 particles were seen on the wear surface of the 50% Al_2O_3 sample under lower forces indicating good bond strength between the particles. The MML layer helps to increase the wear resistance of the composite.
5. EDAX analysis indicated the presence of iron and carbon as separated particles in 50% Al_2O_3 composite. The amount of iron in the valleys was more than the MML layer.

Declaration of conflicting interests

The authors declared no potential conflicts of interest with respect to the research, authorship, and/or publication of this article.

Funding

The authors received no financial support for the research, authorship, and/or publication of this article.

ORCID iD

Vahid Pouyafar https://orcid.org/0000-0003-3130-8713

Supplemental material

Supplemental material for this article is available online.

References

1. Shamim FA, Dvivedi A and Kumar P. Fabrication and characterization of Al6063/SiC composites using electromagnetic stir casting process. Proc IMechE, Part E: J Process Mechanical Engineering: 09544089211045796.
2. Sharma P, Khanduja D and Sharma S. Tribological and mechanical behavior of particulate aluminum matrix composites. *J Reinf Plast Compos* 2014; 33: 2192–2202.
3. Stojanović B and Ivanović L. Application of aluminium hybrid composites in automotive industry. *Tehnički Vjesnik* 2015; 22: 247–251.
4. Vignesh Kumar V, Raja K, Ramkumar T, et al. Studies on mechanical property and wear behaviour of AA7075 hybrid composites prepared by a conventional casting method. *Proceedings of the Institution of Mechanical Engineers, Part E: Journal of Process Mechanical Engineering* 2021; 235: 2180–2188.
5. Kumar M AMM, Baskaran V and Ramji KH. Effect of sliding distance on dry sliding tribological behaviour of aluminium hybrid metal matrix composite (AlHMMC): An alternate for automobile brake rotor – A grey relational approach. *Proc Inst Mech Eng, Part J.* 2016; 230: 402–415.
6. Wu Y. *Fabrication of metal matrix composite by semi-solid powder processing*. ProQuest Dissertations Publishing, 2011.
7. Wu Y, Kim G-Y, Anderson IE, et al. Fabrication of Al6061 composite with high SiC particle loading by semi-solid powder processing. *Acta Mater* 2010; 58: 4398–4405.
8. Wu Y and Kim G-Y. Carbon nanotube reinforced aluminum composite fabricated by semi-solid powder processing. *J Mater Process Technol* 2011; 211: 1341–1347.
9. Luo X, Wu M, Fang C, et al. The current status and development of semi-solid powder forming (SPF). *Jom* 2019; 71: 4349–4361.
10. Liu X, Huang C, Zhao L, et al. A comparative study on the friction and wear properties of semi-solid cast A356 alloy. *Int J Mater Res* 2015; 106: 425–428.
11. Radha A, Suresh S, Ramanan G, et al. Processing and characterization of mechanical and wear behavior of Al7075 reinforced with B4C and nano graphene hybrid composite. *Mater Res Express* 2020; 6: 1265c.
12. Bai Y, Guo Y, Li J, et al. Effect of Al_2O_3 nanoparticle reinforcement on the mechanical and high-temperature tribological behavior of Al-7075 alloy. *Proceedings of the Institution of Mechanical Engineers, Part J: Journal of Engineering Tribology* 2017; 231: 900–909.
13. Essa FA, Zhang Q, Huang X, et al. Effects of ZnO and MoS2 solid lubricants on mechanical and tribological properties of M50-steel-based composites at high temperatures: Experimental and simulation study. *Tribol Lett* 2017; 65: 97.
14. Ali MKA and Xianjun H. M50 matrix sintered with nanoscale solid lubricants shows enhanced self-lubricating properties under dry sliding at different temperatures. *Tribol Lett* 2019; 67: 71.
15. Akhtar F, Askari SJ, Shah KA, et al. Microstructure, mechanical properties, electrical conductivity and wear behavior of high volume TiC reinforced cu-matrix composites. *Mater Charact* 2009; 60: 327–336.
16. He X, Liu J and An L. The mechanical behavior of hierarchical Mg matrix nanocomposite with high volume fraction reinforcement. *Materials Science and Engineering: A* 2017; 699: 114–117.
17. Kang H-K. Microstructure and electrical conductivity of high volume Al_2O_3-reinforced copper matrix composites produced by plasma spray. *Surf Coat Technol* 2005; 190: 448–452.
18. Prabhu B, Suryanarayana C, An L, et al. Synthesis and characterization of high volume fraction Al–Al_2O_3 nanocomposite powders by high-energy milling. *Materials Science and Engineering: A* 2006; 425: 192–200.
19. Zheng R, Chen J, Zhang Y, et al. Fabrication and characterization of hybrid structured Al alloy matrix composites reinforced by high volume fraction of B4C particles. *Materials Science and Engineering: A* 2014; 601: 20–28.
20. Alhawari K, Omar M, Ghazali M, et al. Wear properties of A356/Al_2O_3 metal matrix composites produced by semi-solid processing. *Procedia Eng* 2013; 68: 186–192.
21. Pola A, Tocci M and Kapranos P. Microstructure and properties of semi-solid aluminum alloys: A literature review. *Metals (Basel)* 2018; 8: 181.
22. Kok M. Production and mechanical properties of Al_2O_3 particle-reinforced 2024 aluminium alloy composites. *J Mater Process Technol* 2005; 161: 381–387.
23. Rosso M. Ceramic and metal matrix composites: Routes and properties. *J Mater Process Technol* 2006; 175: 364–375.
24. International A. ASTM G99-17. *Standard test method for wear testing with a pin-on-disk apparatus*. ASTM International West Conshohocken, 2017.
25. Sathish T and Karthick S. Wear behaviour analysis on aluminium alloy 7050 with reinforced SiC through Taguchi approach. *Journal of Materials Research and Technology* 2020; 9: 3481–3487.
26. Gul F and Acilar M. Effect of the reinforcement volume fraction on the dry sliding wear behaviour of Al–10Si/SiCp composites produced by vacuum infiltration technique. *Compos Sci Technol* 2004; 64: 1959–1970.
27. Van Thuong N, Zuhailawati H, Anasyida AS, et al. Dry wear behavior of cooling-slope-cast hypoeutectic aluminum alloy. *Int J Mater Res* 2016; 107: 578–585.
28. Fogagnolo J, Velasco F, Robert M, et al. Effect of mechanical alloying on the morphology, microstructure and properties of aluminium matrix composite powders. *Materials Science and Engineering: A* 2003; 342: 131–143.
29. Ray S. Casting of metal matrix composites. In: Newaz GM, Neber-Aeschbacher H and Wohlbier FH (eds) *Key engineering materials*. Trans Tech Publ, 1995, p. 417–446.
30. Chen Y-s, Chen T-j, Zhang S-q, et al. Effects of processing parameters on microstructure and mechanical properties of powder-thixoforged 6061 aluminum alloy. *Transactions of Nonferrous Metals Society of China* 2015; 25: 699–712.
31. Wu Y and Kim G-Y. Compaction behavior of Al6061 powder in the semi-solid state. *Powder Technol* 2011; 214: 252–258.
32. Al-Rubaie KS, Yoshimura HN and de Mello JDB. Two-body abrasive wear of Al–SiC composites. *Wear* 1999; 233: 444–454.

33. Qin S, Chen C, Zhang G, et al. The effect of particle shape on ductility of SiCp reinforced 6061 Al matrix composites. *Materials Science and Engineering: A* 1999; 272: 363–370.
34. Ramakrishnan N. An analytical particulate study on strengthening of reinforced. *Acta Mater* 1996; 44: 69–75.
35. Constantin V, Scheed L and Masounave J. Sliding wear of aluminum-silicon carbide metal matrix composites. *J Tribol* 1999; 121: 787–794.
36. Wilson S and Alpas A. Wear mechanism maps for metal matrix composites. *Wear* 1997; 212: 41–49.
37. Hashempour M, Razavizadeh H and Rezaie H. Investigation on wear mechanism of thermochemically fabricated W–Cu composites. *Wear* 2010; 269: 405–415.
38. Riahi A and Alpas A. The role of tribo-layers on the sliding wear behavior of graphitic aluminum matrix composites. *Wear* 2001; 251: 1396–1407.
39. Venkataraman B and Sundararajan G. Correlation between the characteristics of the mechanically mixed layer and wear behaviour of aluminium, Al-7075 alloy and Al-MMCs. *Wear* 2000; 245: 22–38.